ANTENNAS INTEGRATED WITH SOLAR ARRAYS
FOR SPACE VEHICLE APPLICATIONS

J. Huang* and M. Zawadzki

Jet Propulsion Laboratory
California Institute of Technology
Pasadena, California 91109, USA

Introduction: As space vehicles become smaller, real estate for allocating the vehicles' instruments and components becomes a premium quantity. On the other hand, almost all space vehicles require at least one large-aperture solar array and one large-aperture telecommunication antenna in order to maintain an adequate amount supply of power and a robust communication link. One solution to reduce the burden of these two large apertures on the space vehicles is to combine these two structures. This will achieve the critical goals of reducing the space vehicle's mass, stowage volume, and deployed surface area. This will also facilitate the vehicle's maneuverability and attitude control, and increase the field of view of other scientific instruments. Although both the antenna and the solar array can be very thin in profile and low in mass, they separately require massive and large support panels to maintain their required aperture surface tolerance. By combining the two apertures, one support structure can thus be eliminated. The performance of the antenna and solar array both vary with the cosine of the angle from their broadside directions. This would allow significant mission flexibility and the potential to optimize the pointing angle of the integrated array between the Sun and the Earth. Most deep-space missions have Sun/Earth subtended angles of less than 40°. If an integrated array were pointed half-way between the Sun and the Earth with a 40° subtended angle, this would represent only a 0.5dB loss for the antenna and a 6% reduction in solar array output.

This paper presents the results of two antenna/solar array integrations. In both designs, the printed microstrip radiator, due to its small size and low profile, was selected as the element for the antenna array to be integrated with the solar array. An earlier attempt to integrate a single microstrip patch with several solar cells was carried out successfully at S-band frequency [1]. The first antenna/solar array integration presented here uses a low-gain UHF crossed-slot microstrip radiator [2] for future Mars rover application. The second integration uses a high-gain microstrip reflectarray at X-band [3,4] for future deep-space telecom application.

UHF low-gain antenna: The objective of this task was to develop low-mass, compact, omni-directional, UHF antennas for future Mars rover application. The antenna was required to have a wide beamwidth (±60° conical coverage) so that it can communicate with an orbiting satellite that flies by horizon-to-horizon in any orbital track. The antenna should be a single unit operational over both the downlink (401 MHz) and the uplink (437 MHz) frequencies (separated by 8.5% bandwidth) with circular polarization (CP) and a minimum gain of −2 dBi over the ±60° angular region. It was required to have a mass less than 0.5 kg and a size compact enough so as not to significantly obscure or reduce the area allocated for the solar panel (50cm x 80cm). It is clear that this antenna task is quite challenging. A broad angular coverage with CP generally calls for a physically tall antenna so that it has adequate aperture size to provide close-to-the-horizon coverage. However, such a tall antenna would shadow the solar cells. On the other hand, a low-profile antenna at UHF would have a large physical aperture (half free-space wavelength is about 35cm), which may take significant area away from that allocated for the solar cells. In addition, the antenna requires either a relatively large bandwidth or a dual-frequency capability, which implies that the electrical size of the antenna could be difficult to miniaturize. After a trade-off study, the crossed-slot microstrip patch [5], shown in Fig. 1, was selected for breadboard development. This is because of its ability to radiate a relatively broad beam, to integrate with the solar array, and to achieve very small mass.

The crossed-slot patch is a microstrip antenna element that consists of four ¼-wavelength-long sub-patches. Each sub-patch has a square or slightly rectangular shape. The four sub-patches are shorted to the ground plane at four sequentially located edges. The four sub-patches are sequentially oriented with 0°, 90°, 180°, 270° electrical phase excitations. The four sub-patches are separated from and supported above the ground plane by a 2.5cm thick dielectric honeycomb panel. Since a sub-patch radiates only from its three open edges, foreign low-profile objects (metallic or nonmetallic) can be placed on top of each sub-patch without significantly disturbing the radiation characteristics of the antenna. Consequently, solar cells can be placed on top of the four sub-patches as sketched in Fig. 2. A conceptual drawing of the antenna mounted on a Mars rover is shown in Fig. 3. With this antenna concept, only 6.5% of the total solar-panel area is lost due to the antenna, while the antenna's electrical aperture takes about 25% of the total solar panel area. The input return loss of the antenna, when integrated with the solar panel, was measured to be −10dB or less across the required bandwidth of 40 MHz. The measured radiation patterns in the two principal planes of the integrated array are given in Figs. 4(a) and 4(b). These patterns indicate the achievement of the needed broad beam radiation. The measured peak gain is 4.5 dBic at the two required frequencies.

X-band high-gain antenna: The objective of this task was to develop a 0.5m high-gain CP X-band antenna integratable with a solar array. The antenna selected was a printed microstrip reflectarray with crossed-dipoles as the radiating elements. It was selected based on three key reasons: 1) the reflectarray elements do not require a power division network, which makes the integration much more feasible than a conventional array antenna; 2) it has a flat aperture which is amenable to integration with a flat solar panel; 3) the crossed-dipoles are physically very thin and do not significantly block the sunlight to the solar cells situated below the RF elements. The reflectarray in this design consists of 408 X-band crossed-dipole elements. The element spacing is 0.56 free-space wavelengths at 8.4 GHz and was chosen to fit the solar cell size of 2cm x 4cm. This yields an integer number of 2 crossed-dipoles per solar cell. Fig. 5 shows a photograph of the final integrated antenna/solar array structure, and Fig. 6 gives the cross-section sketch of the integrated array with a top view of a single solar cell. A tripod strut assembly was used to hold a circularly-polarized conical feed horn with a 3dB-beamwidth of 39° and a −9dB edge taper to the reflectarray aperture. The f/D ratio of the antenna is 0.75. The 204 solar cells were secured onto the anodized aluminum plate with a silicon-based adhesive. A 1.52mm-thick coverglass, which serves to protect the solar cell, was bonded to the top of each cell. This coverglass also provides the required vertical separation between the solar cells and the dipoles. The printed crossed-dipoles were etched onto a sheet of 0.051mm-thick Kapton membrane, and secured to the top of the coverglasses with a silicon-based adhesive. Even though Kapton does absorb a significant amount of light energy, it was chosen because it was readily available in large quantities with a thin copper coating that is easily etched. Polymers with high optical transparency should be used in the future for actual implementation of the integrated array.

The measured solar array results were very good. The addition of the dipoles only reduced the electrical output by about 10%. This loss of power could be easily regained by increasing the area of the solar array by 10%, or by increasing the diameter by only 5%. This is a very small amount considering the overall reductions of mass and volume realized by combining the RF and solar arrays. The result for the antenna, while encouraging, was not as good. The measured radiation pattern, shown in Fig. 7, indicates that the reflectarray did form a good coherent beam in the far field; however, the measured aperture efficiency was only about 10% - far from the expected value of 40%. This relatively low efficiency is likely the result of two main factors. First, the electrical characteristics of the overall dipole substrate and the inhomogeneous ground plane were not well-understood or well-considered in the design, mainly because the fine and inhomogeneous silver grid on the top surface of the solar cells is difficult to characterize. The second factor has to do with the reflectarray element itself. It was felt that elements other than crossed-dipoles should be examined in an attempt to find an optimal and more efficient element. Future work to improve the RF efficiency would focus on these two areas. Nevertheless, the results of this development indicate that the integration of large antenna and solar array apertures is highly feasible.

References:

1. M. Tanaka, R. Suzuki, Y. Suzuki, and K. Araki, "Microstrip antenna with solar cells for microsatellites," IEEE AP-S symposium, June 1994, pp. 786-789.
2. J. Huang, "Mars rover antenna for solar-array integration," JPL TMO Progress Report 42-136, Feb. 1999, pp. 1-13.
3. J. Huang, "Capabilities of printed reflectarray antennas," IEEE Phased Array Systems and Technology Conference, Boston, Massachusetts, Oct. 1996, pp. 131-134.
4. M. Zawadzki and J. Huang, "Integrated RF antenna and solar array for spacecraft application," IEEE Phased Array Systems & Technology Conference, Dana Point, California, to be published in May 2000.
5. G. G. Sanford and L. Klein, "Recent developments in the design of conformal microstrip phased arrays," IEE Conf. Publ. 160, Maritime and Aeronautical Satellites for Communication and Navigation, London, 1978, pp. 105-108.
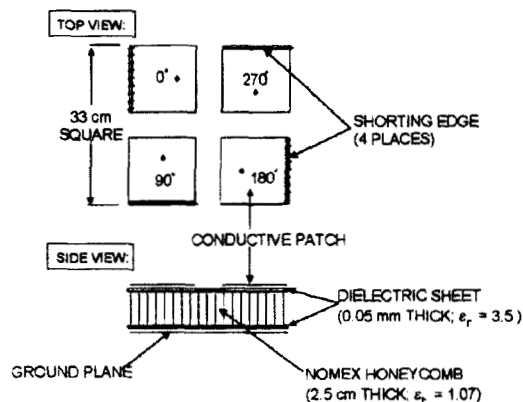
Figure 1. Crossed-slot microstrip patch
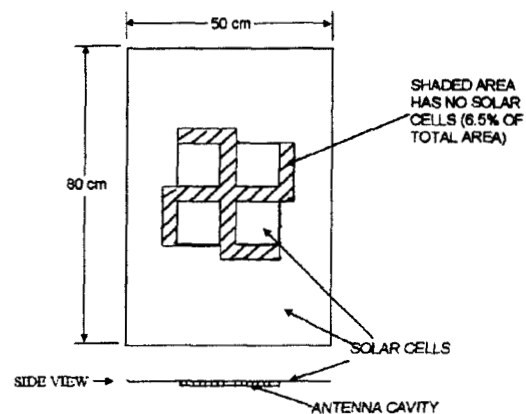
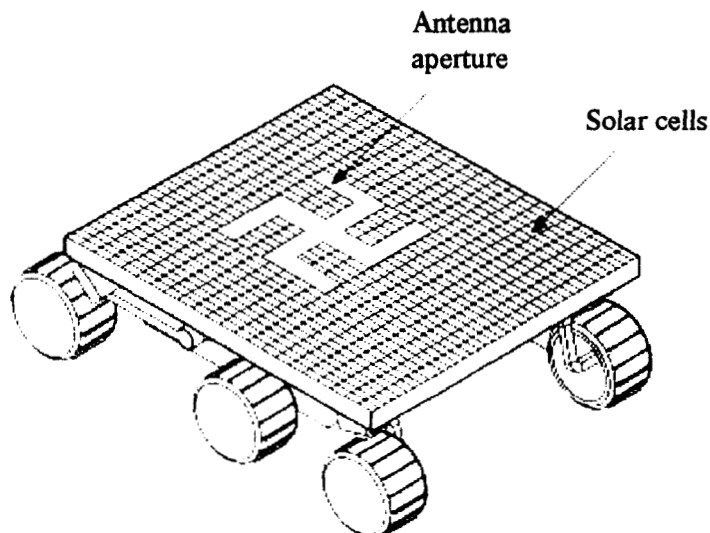Figure 2. Sketch of crossed-slot patch integrated with the solar panel

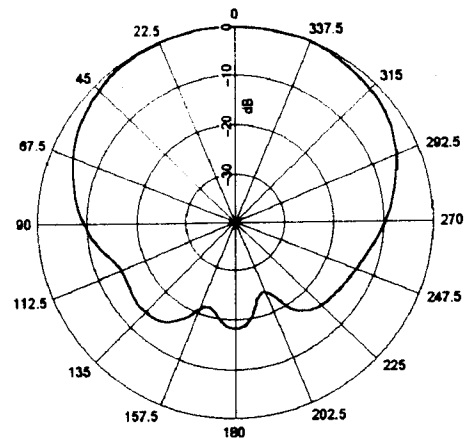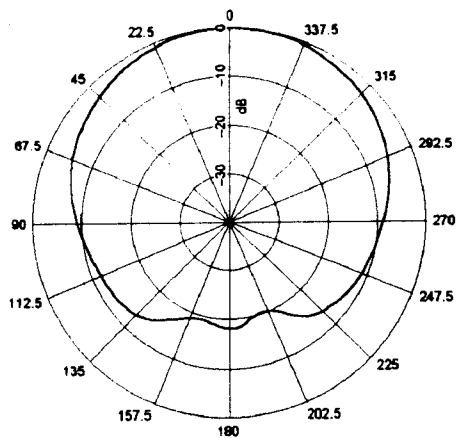Figure 3. Antenna integrated with solar panel On Mars rover

Figure 4. The measured principal-plane patterns of the crossed slot antenna mounted
as in Figure 2: (a) along the narrow dimension of the panel and (b) along the
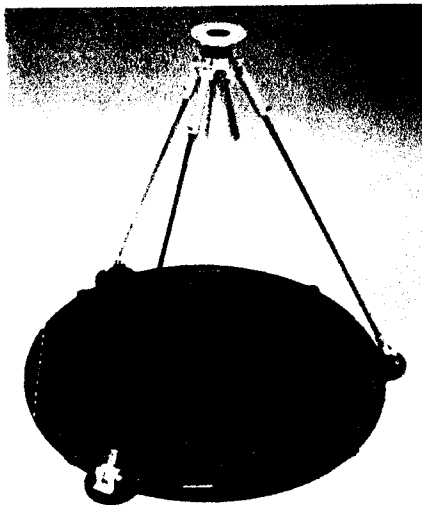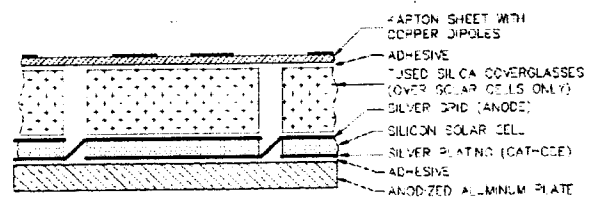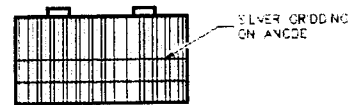broad dimension of the panel.

Figure 5. Integrated antenna/solar array

Figure 6. Cross-section of antenna and top
view of solar cell

Figure 7. Measured radiation
pattern of the integrated antenna
at 8.5 GHz